

Design of compact dual-resonance multiple-input-multiple-output antenna array for internet of things application

Mahesh Kadu¹, Pankaj Pramod Chitte², Sandip R. Udawant³, Vilas S. Ubale⁴

¹Department of Electronics and Telecommunication Engineering, Faculty of Engineering, Amrutvahini College of Engineering, Maharashtra, India

²Department of Electronics and Computer Engineering, Faculty of Engineering, Pravara Rural Engineering College, Maharashtra, India

³Department of Electronics and Telecommunication Engineering, Faculty of Engineering, Dr. Vithalrao Vikhe Patil College of Engineering, Maharashtra, India

⁴Department of Electronics and Computer Engineering, Faculty of Engineering, Amrutvahini College of Engineering, Maharashtra, India

Article Info

Article history:

Received Feb 6, 2025

Revised Sep 30, 2025

Accepted Oct 14, 2025

Keywords:

Antenna array

Compact

Dual-resonance

Electromagnetic band-gap

Internet of things

ABSTRACT

This work presents a compact dual-resonance multiple-input-multiple-output (MIMO) antenna array for internet of things (IoT)-enabled smart devices requiring both 5G and Wi-Fi connectivity. The antenna operates at 3.6 GHz (5G smartphones) and 5.4 GHz (high-speed Wi-Fi), using a dual-resonance MIMO configuration for reliable multi-device communication. An integrated electromagnetic band-gap (EBG) structure suppresses surface waves, reducing mutual coupling and achieving >35 dB isolation with an envelope correlation coefficient (ECC) of 0.05. A fabricated prototype validated the design, with measurements aligning closely with simulations. The proposed antenna offers compactness, dual-band operation, low coupling, and strong MIMO performance, making it well-suited for next-generation IoT systems.

This is an open access article under the [CC BY-SA](#) license.



Corresponding Author:

Mahesh Kadu

Department of Electronics and Telecommunication Engineering, Faculty of Engineering

Amrutvahini College of Engineering

Sangamner, Maharashtra, India

Email: mahesh.kadu@gmail.com

1. INTRODUCTION

Internet of things (IoT)-enabled automation technology is rapidly evolving in the field of communication. A key benefit of this technology is its capability to manage and monitor multiple devices and systems from a centralized platform, such as a smartphone or tablet [1]. Furthermore, smart devices can communicate with each other through wireless protocols like Wi-Fi. To facilitate dual communication in such smart devices, the antenna system should be a dual-resonance multiple-input-multiple-output (MIMO) antenna array system [2]. However, in IoT environments where compact smart devices host multiple wireless applications, space constraints pose challenges for integrating antenna array elements [3]. This necessitates the design of compact dual-resonance antenna arrays, which lead to more space-efficient solutions [4]. A compact antenna, serving as an array element, enables the realization of smaller antenna arrays. Various methods for designing dual-resonance antennas are discussed by the researchers. For instance, the coplanar waveguide feeding technique has been explored in [5], for achieving dual-resonance operation in rectangular patches, though this method suffers from higher losses compared to other approaches. Fractal antenna design is a widely used approach for enabling dual-resonance in patch elements [6]. Several resonances are generated in the fractal antenna, allowing a dual-resonance operation. However, this approach can produce unwanted resonant frequencies and does not allow for independent tuning of each frequency band. Multiple

patches have been integrated into single antenna design to achieve dual-resonance operation as reported in [7], but connecting individual patch elements for independent tuning often results in larger antenna sizes. Other methods, such as truncating patch corners [8], using metamaterials [9], or incorporating frequency-selective surfaces (FSS) [10], have also been investigated. While these techniques show promise, they come with limitations, such as increased design complexity, difficulty in replicability, and large dimensions, which are unsuitable for compact IoT devices. Slot incorporation in patch elements can achieve dual-resonance functionality [11], but it may reduce the antenna's gain. Similarly, monopole antennas have been adapted for dual-resonance operation [12], but ensuring precise resonance frequencies remains a challenge. Overall, many dual-resonance antenna designs reported in the literature are either too large, complex, or lack the ability to independently tune frequency bands, making them less practical for IoT-based wireless applications. The findings are summarized in Table 1.

Table 1. Summary of dual-resonance techniques

Technique	Advantages	Limitations	Suitability for IoT
Coplanar waveguide (CWP) feeding	Enables dual-resonance in rectangular patches, planar structure	Higher losses, limited efficiency	Comparatively it has more losses
Fractal antenna	Compact geometry	Produces unwanted resonant frequencies, no independent tuning of bands	Moderately suitable, tuning limitations
Multiple patch integration	Allows dual-resonance operation, potential for independent tuning	Increases overall antenna size, complex interconnection	Poor fit for compact IoT applications
Corner truncation of patch	Simpler design modification can shift resonance	Limited tuning range, may affect radiation pattern	Partially suitable, limited control over frequency
Metamaterials	High design flexibility, enhances miniaturization and bandwidth	Complex design and fabrication, replication issues	Complex for mass deployment in IoT
FSS	Can improve bandwidth	Increases antenna size	Not compact enough for IoT
Slot incorporation in patch	Enables dual-resonance, easier integration in planar design	Requires careful optimization	Suitable with controlled optimization
Monopole antennas with modifications	Compact, simple structure	Precise tuning is difficult, limited control over dual bands	Compact but less frequency control

Closely spaced antenna elements within an antenna array often experience mutual coupling, which can significantly degrade the array's performance [13]. Various techniques have been developed to mitigate mutual coupling in MIMO antenna arrays. One such technique is the defected ground structure (DGS) [14], where specific slot shapes are etched into the ground surface to reduce mutual coupling. However, incorporating DGS into antennas with a full ground surface may reduce the total gain and efficiency of the antenna with DGS. Another approach involves using metamaterials to suppress surface waves, thereby improving isolation in multi-antenna systems [15]. Despite their effectiveness, the application of metamaterials is limited by their high cost and limited availability. Stub elements can also be used to reduce mutual coupling [16], although the level of improvement achieved is relatively minor. Neutralization lines, which connect adjacent antenna elements [17], are effective in canceling mutual coupling but add complexity to the array design. An electromagnetic band-gap (EBG) structure is another popular method for enhancing isolation in antenna arrays [18]. EBG structures act as bandstop filters and are known to provide higher isolation levels compared to other techniques. Additionally, they are relatively simple to design, making them an attractive solution for reducing mutual coupling in MIMO antenna arrays. Shorting pins are also used to minimize mutual coupling currents between ports [19], but they require precise design to avoid adverse effects on other antenna parameters. The comparison of mutual coupling reduction techniques is presented in Table 2.

This work aims to design a compact dual-resonance MIMO antenna array that supports dual frequency bands for IoT applications with reduced mutual coupling. The array is constructed using an economical FR4 substrate and operates at dual frequencies of 3.6 GHz and 5.4 GHz. These dual-resonance operations are achieved by incorporating a ground slot and a stub, allowing independent tuning of each frequency band. To minimize mutual coupling among antenna elements, an additional EBG element is integrated into the antenna array. The methodology used in this research is detailed in section 2. The design of a compact dual-resonance antenna is described in section 3. The development of the dual-resonance antenna array with EBG is covered in section 4. Section 5 discusses the testing and results of the fabricated antenna array prototype, while section 6 concludes the findings of the study.

Table 2. Comparison of mutual coupling reduction techniques

Technique	Working principle	Advantages	Limitations
DGS	Etching specific slot shapes into the ground to disturb current distribution and reduce coupling.	Simple to implement; effective mutual coupling suppression.	Can reduce total gain and efficiency due to disrupted ground continuity.
Metamaterials	Use of engineered structures to suppress surface waves and prevent mutual interaction.	High isolation; effective over a broad frequency range.	High cost and limited availability restrict widespread use.
Stub elements	Placement of resonant stubs between elements to cancel coupling-induced currents.	Easy fabrication; low implementation cost.	Offers only marginal improvement in isolation.
Neutralization lines	Direct connection between adjacent elements to cancel induced mutual coupling currents.	Highly effective for reducing coupling between closely spaced elements.	Increases design complexity and may affect impedance matching.
EBG structures	Periodic structures that act as bandstop filters to suppress surface waves.	Provides high isolation; relatively easy to design and integrate.	Requires careful design and optimization for specific frequency bands.
Shorting pins	Vertical conductive vias connecting the patch to the ground to divert mutual currents.	Effective for compact arrays; enhances port isolation.	Requires precise placement to avoid negatively affecting radiation performance.

2. METHOD

The method employed for the development of the small-size dual-resonance MIMO antenna array is illustrated in Figure 1. Following these design steps allows the designer to develop a low mutual coupling dual-resonance antenna array for the desired frequency applications. This process can act as a guide for researchers aiming to adapt the proposed antenna array design to other wireless frequency applications.

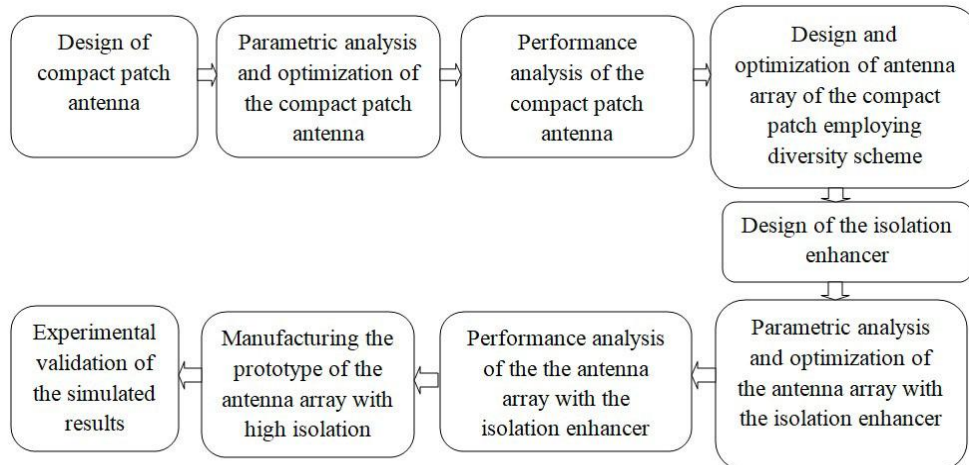


Figure 1. Design method

The design process of a compact patch antenna begins with the selection of a suitable substrate material, considering its dielectric constant (ϵ_r) and loss tangent ($\tan \delta$), as these parameters significantly influence the antenna's size, efficiency, and overall performance. A substrate with a higher dielectric constant helps in reducing the physical size of the antenna, making it ideal for compact applications. Once the substrate is chosen, the next step involves determining the operating frequency and using standard microstrip antenna design equations to calculate the initial patch dimensions such as width and length. An appropriate feeding technique is then selected based on the compactness and performance requirements of the design.

A variety of methods have been explored to achieve dual-resonance in compact antenna designs, particularly for array applications [20]. Select one of the method suitable for user application. The optimization of a compact dual-resonance patch antenna involves performing parametric analysis using a simulation tool like high-frequency structure simulator (HFSS). Key design parameters such as patch dimensions, slot size, feed position, and substrate height are defined as variables. These are systematically varied to study their impact on performance metrics like return loss and resonance frequencies. An optimization routine is then applied to achieve the desired dual-resonance behavior with good impedance

matching. This approach ensures a compact, high-performance antenna design suitable for modern wireless applications.

Arrange multiple patch elements in a suitable configuration (linear or planar), ensuring adequate spacing to minimize mutual coupling. Incorporate coupling reduction techniques such as DGS, EBG structures, or isolation slots. Choose an appropriate feeding method (e.g., microstrip or coaxial) and ensure proper impedance matching. Simulate the array using tools like HFSS to analyze return loss, isolation, gain, and MIMO performance metrics such as envelope correlation coefficient (ECC) and diversity gain (DG). Finally, fabricate and test the prototype, and optimize the design based on measured results. To validate the simulated performance of the MIMO antenna array, begin by measuring the S-parameters using a vector network analyzer (VNA) and compare them with the HFSS simulation results. Conduct radiation pattern measurements in an anechoic chamber or open-area test site to assess real-world behavior.

3. COMPACT DUAL-RESONANCE ANTENNA

Initially, a simple single resonance antenna, operating at 5.4 GHz and fed through a microstrip line, was designed using established design equations given in [21]. This single-resonance antenna is then modified to yield a dual-resonance antenna by integrating a stub element, as illustrated in Figure 2. Figure 2(a) depicts the top view of the proposed antenna and Figure 2(b) presents the bottom view of the dual-resonance antenna. To further improve the dual-resonance performance patch and ground slot were added. The ground slot was etched below the position of the stub. The compact dual-resonance antenna is analyzed through parametric analysis. The final dimensions of the dual-resonance antenna are summarized in Table 3.

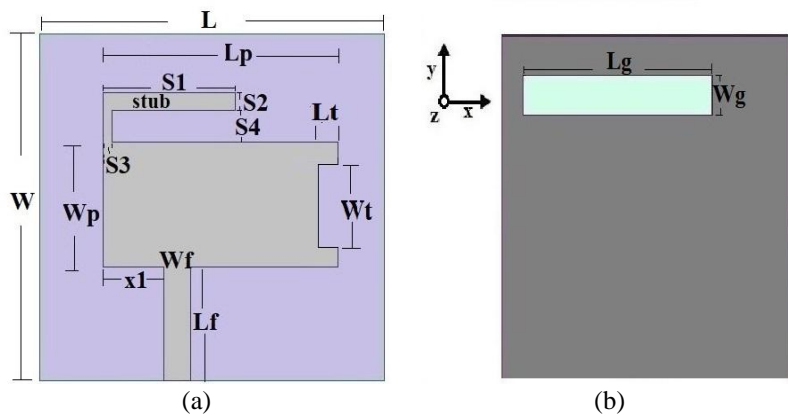


Figure 2. Dual-resonance antenna; (a) top view of the patch and (b) bottom view revealing the ground slot located on the underside of the antenna

Table 3. Dimensions of dual-resonance antenna

Parameter	W_p	L_p	W	L	W_f	L_f	X_1	S_1	S_2	S_3	S_4	W_t	L_t	L_g	W_g
Dimensions (mm)	7	14	20	20	6.5	2	3.5	7	1	0.5	2	4	1.5	13	2.2

3.1. Parametric analysis

The ability of the dual-resonance antenna to independently tune its two frequencies is verified through a parametric analysis as illustrated in Figure 3. The results, presented in Figure 3(a), illustrate how the resonant frequency shifts in response to variations in the width of the horizontal stub arm (S_2). It was observed that the return loss at 3.6 GHz frequency is significantly affected by changes in S_2 , whereas the 5.4 GHz frequency remains largely unaffected. This verifies that the 3.6 GHz resonance component is independently tuned by tuning the dimensions of S_2 .

The impact analysis of the ground slot width (W_g) variation on both frequency bands is depicted in Figure 3(b). The analysis reveals that resonance components centered at 3.6 GHz do not show any variations by change in the value of W_g . While the variation in the ground slot width varies the frequency components at the 5.4 GHz frequency band. It indicates that the ground slot width independently tunes the 5.4 GHz frequency band.

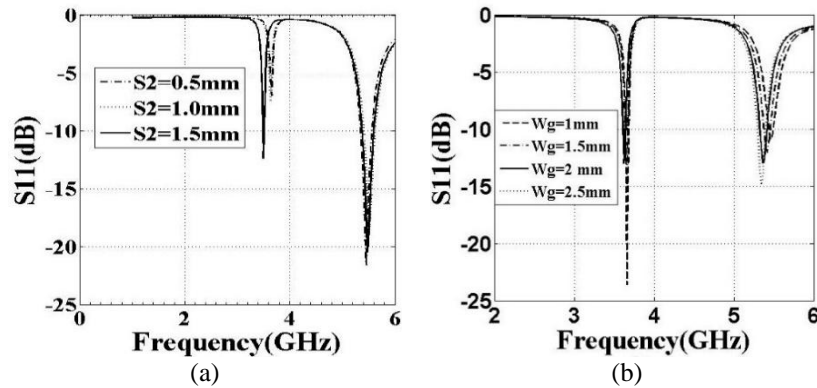


Figure 3. Independent tuning of the dual-resonance frequency bands; (a) at 3.6 GHz and at 5.4 GHz

4. COMPACT DUAL-RESONANCE ANTENNA ARRAY WITH ELECTROMAGNETIC BAND-GAP

The compact dual-resonance antenna array with EBG is depicted in Figure 4(a). It features symmetric placement of two identical compact dual-resonance antenna elements at a specified distance (d)=12 mm from each other. Due to limited space for placing the antenna array within a portable wireless device, the two antenna elements are closely positioned. The mushroom EBG structure reduces the mutual-coupling within the antenna array. Low mutual-coupling is crucial for the effective performance of an antenna array. A mushroom EBG was designed and positioned at the center of the antenna array, as shown in Figure 4(a). The EBG structure was optimized with patch dimensions of $e_1=e_2=4$ mm, and the via radius r was fixed at 0.7 mm, calculated using design equations given in [22]. The three EBG elements act as a stopband filter. The separation distances $m=2$ mm and $t=2$ mm along the y-axis and x-axis, respectively, between the EBG elements, were optimized for optimal performance. The array has an overall width (W)=20 mm and length (L)=50 mm.

Figure 4(b) showcases a 4 dB improvement in isolation compared to the isolation level measured without EBG. The proposed dual-resonance antenna array with EBG showcases a mutual coupling of 36 dB and 37 dB at 3.6 GHz and 5.4 GHz frequency respectively.

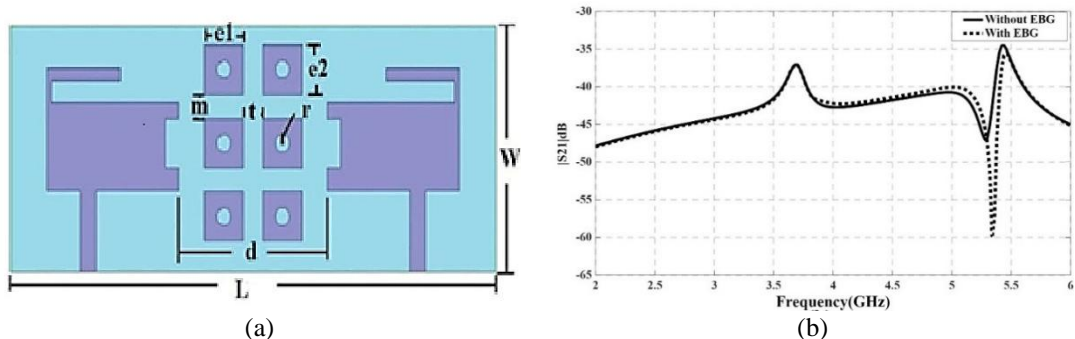


Figure 4. Compact dual-resonance antenna array with EBG; (a) top view and (b) effect of EBG on mutual-coupling

5. RESULTS AND DISCUSSION

The compact dual-resonance antenna array with EBG, designed with the optimized dimensions outlined in section 4, was fabricated, as shown in Figure 5(a). Figure 5 exhibits the manufactured prototype and its return loss characteristics. The prototype was tested using a VNA to extract S-parameters. The performance of the proposed antenna array was validated by obtaining the measurement results discussed in this section.

5.1. Return loss

The S11 parameter was evaluated using a 2-port network analyzer. As illustrated in Figure 5(b), the test values of the return loss are in good agreement with simulated values at both frequency bands. However, minor discrepancies in the measured reflection coefficient values compared to the simulated results are evident, which can be attributed to slight manufacturing imperfections.

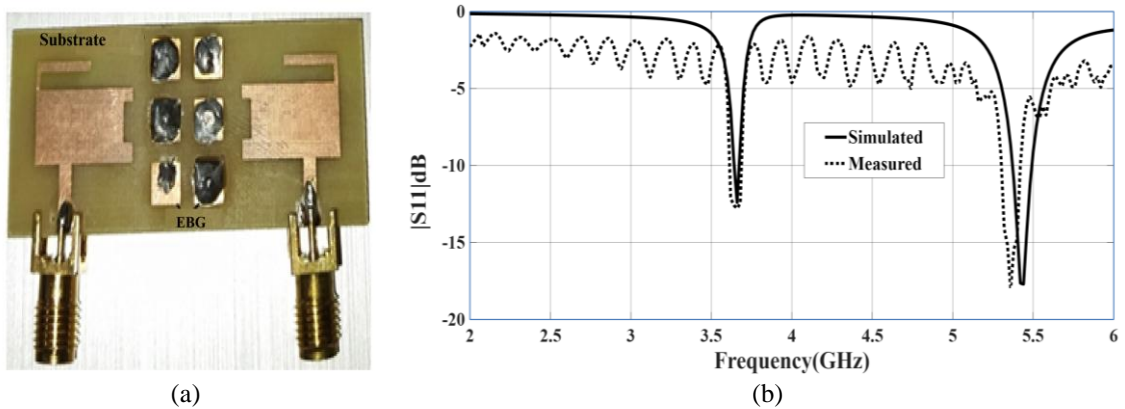


Figure 5. Return loss of manufactured prototype; (a) manufactured prototype and (b) variation of return loss with frequency for the manufactured prototype

5.2. Mutual coupling

The mutual coupling between the antenna elements in the proposed array with EBG was measured. The measured S21 values were obtained using the two-port network analyzer, while the simulated inter-port coupling coefficients were generated using HFSS simulation software. Figure 6 presents the plots of the coupling coefficients (S21) with the variation in the frequency, both the plot shows matching at both the frequency components. The isolation remains below 35 dB for both frequency bands. However, minor deviations in the measured values compared to the simulations, can be attributed to connector and manufacturing losses.

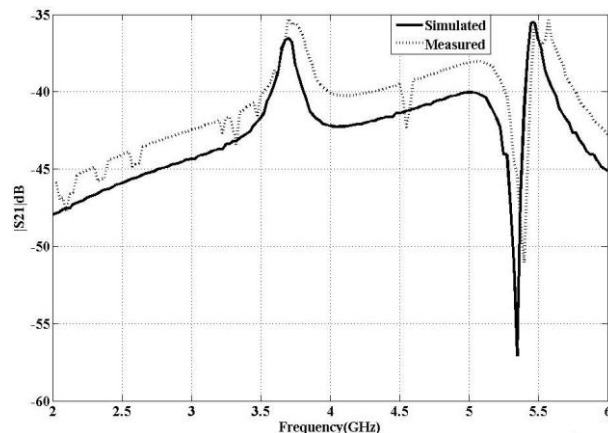


Figure 6. Mutual-coupling variation with frequency

5.3. Radiation pattern and gain

The radiation properties of the designed antenna are illustrated in Figure 7. Figure 7(a) compares the E-plane ($\phi=0^\circ$) radiation characteristics at 3.6 GHz, while Figure 7(b) presents the H-plane ($\phi=90^\circ$) radiation properties at the same frequency. Additionally, Figures 7(c) and (d) depict the E-plane and H-plane radiation properties at 5.4 GHz. The results demonstrate that the antenna maintains stable radiation characteristics at both frequencies, achieving a gain of 2.2 dB at 5.4 GHz and 1 dB at 3.6 GHz.

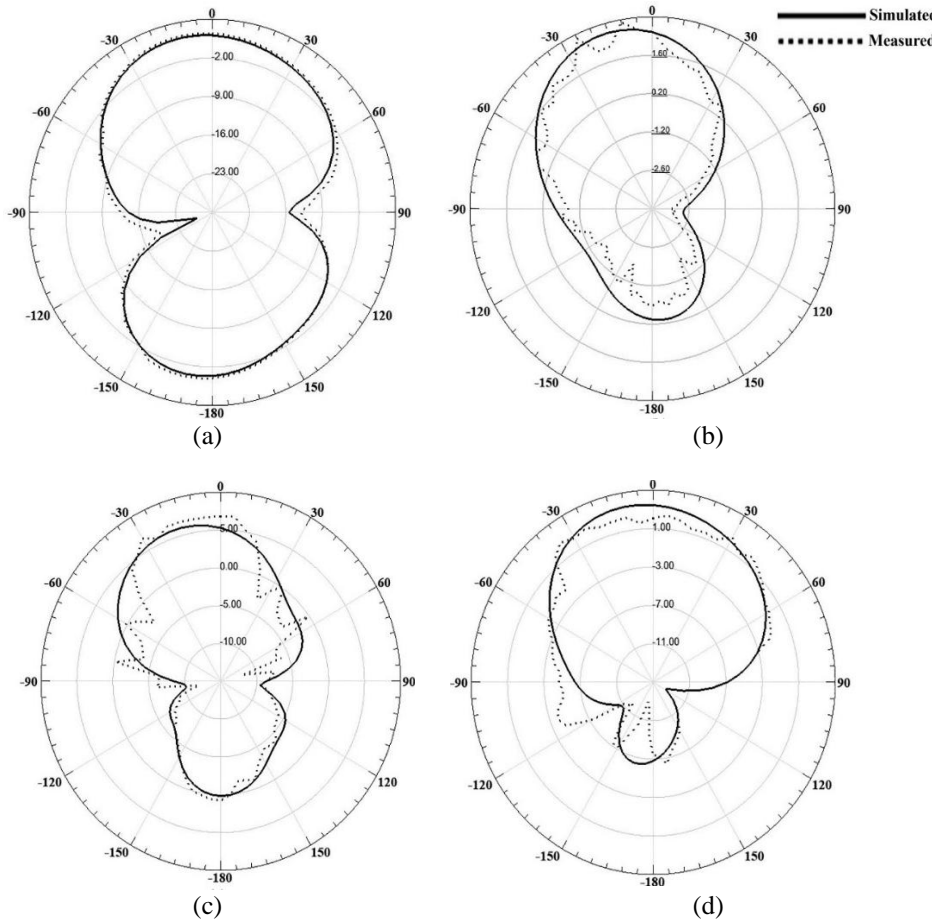


Figure 7. Radiation characteristics; (a) E-plane at 3.6 GHz, (b) H-plane at 3.6 GHz, (c) E-plane at 5.4 GHz, and (d) H-plane at 5.4 GHz

5.4. Envelope correlation coefficient

The ECC provides insight into the mutual-coupling level between the antenna elements. Using (1), the ECC is calculated from S parameters to be 0.05 at 3.6 GHz and 0.07 at 5.4 GHz, indicating satisfactory MIMO performance.

$$ECC = \frac{|S_{11}^*S_{12} + S_{21}^*S_{22}|}{(1 - |S_{11}|^2 - |S_{21}|^2) \times (1 - |S_{21}|^2 - |S_{12}|^2)} \quad (1)$$

5.5. Total active reflection coefficient

Total active reflection coefficient (TARC) is another important parameter for evaluating the MIMO performance of an antenna array in MIMO applications. The TARC values, derived from the measured and simulated S-parameters using (2). Both measured and simulated TARC values are below the threshold of 35 dB for both frequency bands, demonstrating satisfactory MIMO performance.

$$TARC = \frac{\sqrt{(|S_{11} + S_{12}e^{j\theta}|^2) + (|S_{21} + S_{22}e^{j\theta}|^2)}}{\sqrt{2}} \quad (2)$$

5.6. Diversity gain

Diversity between antenna elements in an antenna array is a critical requirement for MIMO applications. The level of diversity is quantified by measuring the DG. Calculated from the ECC value using (3), the DG is 9.9 dB at both 3.6 GHz and 5.4 GHz, indicating satisfactory MIMO performance across both frequency bands.

$$DG = 10 \times \sqrt{(1 - |0.99ECC|^2)} \quad (3)$$

5.7. Comparison with reported designs

The proposed antenna array is compared with reported designs from the literature, as shown in Table 4. Where λ_0 represents the free space wavelength corresponding to highest frequency band of operation of the antenna array. The proposed antenna array features a compact dual-resonance design, achieves significantly higher isolation, and independent tuning capabilities compared to its counterparts.

Table 4. Comparison with reported designs

Parameter/ references	Size	Substrate	Decoupling mechanism	Dual-resonance tuning	Mutual coupling (dB)	ECC
[23]	$2.9 \lambda_0 \times 1.47 \lambda_0$	FR4	Self	Non-independent	15	0.02
[24]	$0.27 \lambda_0 \times 0.47 \lambda_0$	FR4	Stub-loading	Non-independent	21	0.004
[25]	$3.75 \lambda_0 \times 1.87 \lambda_0$	FR4	DGS	Independent	12	0.18
[26]	$3.18 \lambda_0 \times 2.32 \lambda_0$	Rogers RO4003	DGS	Non-independent	18	0.007
[27]	$2.5 \lambda_0 \times 1.25 \lambda_0$	FR4	Self	Non-independent	25	0.17
Proposed	$0.90 \lambda_0 \times 0.36 \lambda_0$	FR4	EBG	Independent	>35	0.05

6. CONCLUSION

In this work, a compact dual-resonance MIMO antenna array has been successfully designed and demonstrated for IoT-based wireless communication systems. The antenna exhibits resonant behavior at 3.6 GHz and 5.4 GHz, catering to dual-band operation with excellent MIMO performance metrics, including low mutual coupling and high port isolation. The measured results closely align with the simulated data, validating the design's accuracy and robustness. Notably, the antenna maintains a compact footprint while offering independent tuning of each frequency band, which enhances its adaptability across different wireless standards.

The proposed design stands out in comparison to existing MIMO solutions, owing to its simplicity, compactness, and superior isolation characteristics making it particularly well-suited for compact device IoT applications. Furthermore, the design's scalability and tunability present opportunities for adaptation to additional frequency bands, supporting future wireless systems.

Looking ahead, the antenna design can be extended to support frequency and pattern reconfigurability through the integration of tunable components. Moreover, miniaturization techniques, flexible materials, and system-level integration with energy harvesting or reconfigurable networks could further enhance its applicability. These directions present a promising scope for future research in developing versatile, high-performance antenna systems for next-generation IoT and wireless communication technologies.

FUNDING INFORMATION

This work is funded under 'Assistance by SPPU for Project-based Innovative Research scheme' by Savitribai Phule Pune University, Pune.

AUTHOR CONTRIBUTIONS STATEMENT

This journal uses the Contributor Roles Taxonomy (CRediT) to recognize individual author contributions, reduce authorship disputes, and facilitate collaboration.

Name of Author	C	M	So	Va	Fo	I	R	D	O	E	Vi	Su	P	Fu
Mahesh Kadu	✓	✓	✓	✓	✓	✓	✓	✓	✓	✓			✓	
Pankaj Pramod Chitte		✓	✓		✓		✓		✓		✓			✓
Sandip R. Udawant	✓					✓		✓		✓	✓			✓
Vilas S. Ubale	✓			✓			✓			✓	✓			✓

C : Conceptualization

I : Investigation

Vi : Visualization

M : Methodology

R : Resources

Su : Supervision

So : Software

D : Data Curation

P : Project administration

Va : Validation

O : Writing - Original Draft

Fu : Funding acquisition

Fo : Formal analysis

E : Writing - Review & Editing

CONFLICT OF INTEREST STATEMENT

Authors state no conflict of interest.

DATA AVAILABILITY

Data availability is not applicable to this paper as no new data were created or analyzed in this study.

REFERENCES

- [1] V. K. Sundari, J. Nithyashri, S. Kuzhaloli, J. Subburaj, P. Vijayakumar, and P. S. H. Jose, "Comparison analysis of IoT based industrial automation and improvement of different processes - Review," *Materials Today: Proceedings*, vol. 45, pp. 2595–2598, 2021, doi: 10.1016/j.matpr.2020.11.338.
- [2] S. Khan *et al.*, "Antenna systems for IoT applications: a review," *Discover Sustainability*, vol. 5, no. 1, pp. 1–27, Nov. 2024, doi: 10.1007/s43621-024-00638-z.
- [3] D. Pacheco-Jardines, G. Leija-Hernández, and L. A. Iturri-Hinojosa, "Double Band MIMO Antenna Design for WLAN, IoT and LTE Applications," *Journal de Ciencia e Ingeniería*, vol. 15, no. 1, pp. 1–9, 2023, doi: 10.46571/jci.2023.1.1.
- [4] Y. Sun, T. Pan, Q. Wang, and F. Huang, "A Dual-Band Compact Four-Port MIMO Antenna Based on EBG and CSRR for Sub-6 GHz Applications," *Progress in Electromagnetics Research Letters*, vol. 105, pp. 17–25, 2022, doi: 10.2528/PIERL22042602.
- [5] H. Liu, L. Meng, X. Huo, and S. Liu, "A Cpw-fed Dual-Band Dual-Pattern Radiation Patch Antenna Based on TM01and TM02Mode," in *2020 9th Asia-Pacific Conference on Antennas and Propagation (APCAP)*, Xiamen, China: IEEE, Aug. 2020, pp. 1–2, doi: 10.1109/APCAP50217.2020.9245936.
- [6] A. N. Alkhafaji, S. M. Abdulsatar, and J. K. Ali, "Design of Flexible Dual-Band Tree Fractal Antenna for Wearable Applications," *Progress In Electromagnetics Research C*, vol. 125, pp. 51–66, 2022, doi: 10.2528/PIERC22062601.
- [7] J. Guo, H. Bai, A. Feng, Y. Liu, Y. Huang, and X. Zhang, "A Compact Dual-Band Slot Antenna with Horizontally Polarized Omnidirectional Radiation," *IEEE Antennas and Wireless Propagation Letters*, vol. 20, no. 7, pp. 1234–1238, Jul. 2021, doi: 10.1109/LAWP.2021.3076169.
- [8] W. W. Chen, Q. S. Wu, and X. Zhang, "Quad-Mode Dual-Band Dual-Sense Circularly Polarized Microstrip Patch Antenna," *IEEE Antennas and Wireless Propagation Letters*, vol. 23, no. 5, pp. 1503–1507, May. 2024, doi: 10.1109/LAWP.2024.3360271.
- [9] J. Xue, G. Wang, S. Li, Z. Wang, and Q. Liang, "A Metamaterial Based Dual-Band UWB Antenna Design for 5G Applications," *Progress In Electromagnetics Research M*, vol. 127, pp. 85–92, 2024, doi: 10.2528/PIERM24042301.
- [10] C. Renit and T. A. B. Raj, "Wearable frequency selective surface-based compact dual-band antenna for 5G and Wi-Fi applications," *Automatika*, vol. 65, no. 2, pp. 454–462, Apr. 2024, doi: 10.1080/00051144.2023.2296796.
- [11] S. Ahmad, A. Ghaffar, N. Hussain, and N. Kim, "Compact dual-band antenna with paired l-shape slots for on-and off-body wireless communication," *Sensors*, vol. 21, no. 23, pp. 1–16, Nov. 2021, doi: 10.3390/s21237953.
- [12] P. Danuor, J. I. Moon, and Y. B. Jung, "High-gain printed monopole antenna with dual-band characteristics using FSS-loading and top-hat structure," *Scientific Reports*, vol. 13, no. 1, pp. 1–12, 2023, doi: 10.1038/s41598-023-37186-x.
- [13] R. S. Parbat, M. B. Kadu, and R. P. Labade, "A Quantitative Solutions and Approaches for Mutual Coupling Reduction in MIMO Antenna," in *2015 Second International Conference on Advances in Computing and Communication Engineering*, Dehradun, India: IEEE, May. 2015, pp. 164–169, doi: 10.1109/ICACCE.2015.34.
- [14] P. Kumar *et al.*, "A defected ground structure based ultra-compact wider bandwidth terahertz multiple-input multiple-output antenna for emerging communication systems," *Heliyon*, vol. 10, no. 17, pp. 1–13, 2024, doi: 10.1016/j.heliyon.2024.e36842.
- [15] A. A. Ibrahim, M. A. Abdalla, and R. M. Shubair, "High-isolation metamaterial MIMO antenna," in *2017 IEEE International Symposium on Antennas and Propagation & USNC/URSI National Radio Science Meeting*, San Diego, CA, USA: IEEE, Jul. 2017, pp. 1737–1738, doi: 10.1109/APUSNCURSINRSM.2017.8072911.
- [16] M. Alibakhshikenari *et al.*, "An innovative antenna array with high inter element isolation for sub-6 GHz 5G MIMO communication systems," *Scientific Reports*, vol. 12, no. 1, pp. 1–13, May. 2022, doi: 10.1038/s41598-022-12119-2.
- [17] Y. Ou, X. Cai, and K. Qian, "Two-element compact antennas decoupled with a simple neutralization line," *Progress in Electromagnetics Research Letters*, vol. 65, pp. 63–68, 2017, doi: 10.2528/PIERL16111801.
- [18] R. Pakala and R. Dasari, "Mutual Coupling Reduction in UWB-MIMO Antenna Using Circular Slot EBG Structures," *Progress In Electromagnetics Research M*, vol. 119, pp. 177–188, 2023, doi: 10.2528/PIERM23080504.
- [19] I. A. Tunio, Y. Mahé, T. Razban, and B. Froppier, "Mutual coupling reduction in patch antenna array using combination of shorting pins and metallic walls," *Progress In Electromagnetics Research C*, vol. 107, pp. 157–171, 2021, doi: 10.2528/PIERC20082803.
- [20] W. A. Awan, T. Islam, F. N. Alsunaydih, F. Alsaleem, and K. Alhassoon, "Dual-band MIMO antenna with low mutual coupling for 2.4/5.8 GHz communication and wearable technologies," *PLoS ONE*, vol. 19, pp. 1–22, 2024, doi: 10.1371/journal.pone.0301924.
- [21] M. B. Kadu, S. B. Deosarkar, and R. P. Labade, "Dual band microstrip patch antenna for MIMO system," in *2015 International Conference on Pervasive Computing: Advance Communication Technology and Application for Society, ICPC 2015*, 2015, doi: 10.1109/PERVASIVE.2015.7087171.
- [22] M. B. Kadu, N. Rayavarapu, and R. P. Labade, "Design of EBG Structure for Mutual Coupling Reduction in Patch Antenna Array," in *2015 International Conference on Pervasive Computing (ICPC)*, Pune, India: IEEE, Jan. 2015, pp. 1–4, doi: 10.1109/PERVASIVE.2015.7087171.
- [23] J. Huang, G. Dong, Q. Cai, Z. Chen, L. Li, and G. Liu, "Dual-band mimo antenna for 5g/wlan mobile terminals," *Micromachines*, vol. 12, no. 5, pp. 1–12, Apr. 2021, doi: 10.3390/mi12050489.
- [24] R. N. Tiwari, P. Singh, B. K. Kanaujia, S. Kumar, and S. K. Gupta, "A low profile dual band MIMO antenna for LTE/Bluetooth/Wi-Fi/WLAN applications," *Journal of Electromagnetic Waves and Applications*, vol. 34, no. 9, pp. 1239–1253, Jun. 2020, doi: 10.1080/09205071.2020.1716859.
- [25] H. Lin, W. Sun, Z. Wang, and W. Nie, "A Dual-Band MIMO Antenna Based on Multimode for 5G Smartphone Applications," *Progress In Electromagnetics Research C*, vol. 148, pp. 31–42, 2024, doi: 10.2528/PIERC24071101.
- [26] G. Saxena *et al.*, "High Isolation Quad-Element SWB-MIMO Antenna with Dual Band-Notch for ISM and WLAN Band Wireless Applications," *Advanced Electromagnetics*, vol. 12, no. 3, pp. 54–60, Sep. 2023, doi: 10.7716/aem.v12i3.2080.

[27] S. Dey and S. Dey, "Dual-band high isolation eight element MIMO antenna using self decoupling technique for 5G smartphone," *International Journal of Microwave and Wireless Technologies*, vol. 16, no. 10, pp. 1756–1771, Dec. 2024, doi: 10.1017/S1759078724001181.

BIOGRAPHIES OF AUTHORS



Dr. Mahesh Kadu completed his graduation in Electronics and Telecommunication Engineering from Pravara Rural Engineering College (PREC) of Savitribai Phule University, India in 2006, and M.Tech. in Electronics and Telecommunication Engineering Dr. BATU in 2011. He was awarded a Ph.D. by Symbiosis International University, India. His research interests are primarily in the area of wireless communications and networks. He can be contacted at email: mahesh.kadu@gmail.com.



Dr. Pankaj Pramod Chitte received a Bachelor of Engineering in Electronics and Telecommunication from SPPU, Pune, India, and a Master of Engineering in Electronics Engineering, from Dr. BAMU, Aurangabad, India, and Ph.D. in Electronics Engineering from Rashtrasant Tukdoji Maharaj University, Nagpur India. Currently, he is the Assistant Professor of the Electronics and Computer Engineering Department of Pravara Rural Engineering College Loni, India. He can be contacted at email: chittepp@pravaraengg.org.in.



Dr. Sandip R. Udawant was born in Maharashtra in 1983. He completed his B.E. in Electronics & Telecommunication Engineering in 2006 and obtained his M.E. in Electronics & Telecommunication in 2012 and completed Ph.D. in 2023. He is currently serving as an Associate Professor & First Year coordinator at Dr. Vithalrao Vikhe Patil College of Engineering, Vilad Ghat, Ahilyanagar, India. His research interests include digital image processing (DIP) and digital communication. He can be contacted at email: udawant_etc@enggnagar.com.



Dr. Vilas S. Ubale did a B.E in Electronics and Telecommunication Engineering from Amravati University in 2002, an M.E in Electronics Engineering from Government College of Engineering, Aurangabad (B.A.M. University) in 2009, and a Ph.D. in Electronics and Communication Engineering from Suresh Gyan Vihar University Jaipur (Rajasthan) in June 2022. His research field area is microwave antenna design. He can be contacted at email: vilas.ubale@avcoe.org.